Journal of Hazardous Materials 462 (2024) 132778

Contents lists available at ScienceDirect

Journal of Hazardous Materials

journal homepage: www.elsevier.com/locate/jhazmat

Research Paper

Migration and emission characteristics of metal pollutants in fluid catalytic cracking (FCC) process

Jiawei Bian [a], Bohan Wang [b], Ximing Niu [c], Hai Zhao [a], Hao Ling [a], Feng Ju [a,d,*]

[a] State Key Laboratory of Chemical Engineering, School of Chemical Engineering, East China University of Science and Technology, Shanghai 200237, China
[b] Key Laboratory of Specially Functional Polymeric Materials and Related Technology of the Ministry of Education, School of Materials Science and Engineering, East China University of Science and Technology, Shanghai 200237, China
[c] Shanghai Research Institute of Chemical Industry CO., LTD, Shanghai 200333, China
[d] Inorganic Chemistry and Catalysis, Debye Institute for Nanomaterials Science, Utrecht University, Utrecht, the Netherlands

HIGHLIGHTS

- Ni, Fe, and V are the main metal pollutants in the FCC flue gas.
- Metals in feed are mainly deposited on catalysts and partially migrated to flue gas.
- Ni is located on the outer layers of catalysts while V penetrates the deep layers.
- Metal distribution affects the migration and emission of metal PM significantly.
- Emission factors of FCC metal PM are developed to supplement emission inventory.

GRAPHICAL ABSTRACT

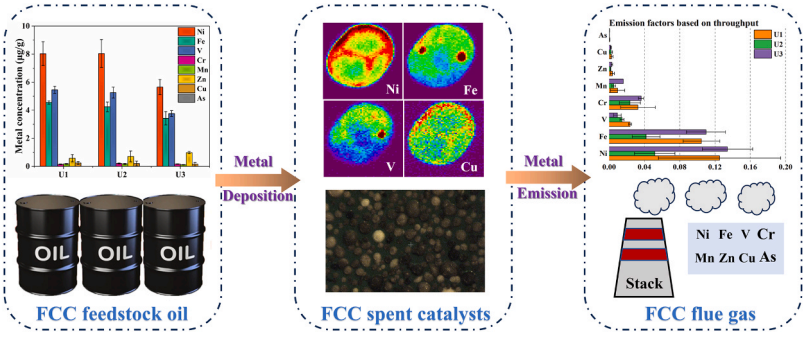

ARTICLE INFO

Editor: Lingxin CHEN

Keywords:
Fluid catalytic cracking
Metal pollutants
Migration rate
Metal distribution
Emission factor

ABSTRACT

Fluid catalytic cracking (FCC) is the core unit for heavy oil conversion in refineries. In the FCC process, the metal contaminants from the feedstock are deposited on the catalysts, causing catalyst deactivation and metal particulate matter (PM) emission. However, the migration and emission characteristics of metal pollutants in FCC units are still unclear. Here, the stack tests of three FCC units were carried out to monitor metal PM emissions, and the metal contents of the feedstock oil and spent catalyst were detected. For the metal migration from the feedstock to the catalysts, Ni, Fe, and V have high concentrations and migration rates while other metals perform much lower. The metal distribution on the spent catalysts profoundly determines the metal mobility to the flue gas and the regeneration process affects the catalyst attrition, leading to metal PM emissions discrepancy. The migration rate and emission concentration of V in the deeper layers of the catalysts are much lower than those of Ni at the particle's exterior. Finally, the stack data was used to calculate the emission factors and ratio factors of the metal PM. This work is expected to advance metal migration cognition and metal pollutants emissions estimation in FCC units.

* Corresponding author at: State Key Laboratory of Chemical Engineering, School of Chemical Engineering, East China University of Science and Technology, Shanghai 200237, China.
E-mail address: jufeng@ecust.edu.cn (F. Ju).

https://doi.org/10.1016/j.jhazmat.2023.132778
Received 16 August 2023; Received in revised form 1 October 2023; Accepted 11 October 2023
Available online 13 October 2023

1. Introduction

Fluid catalytic cracking (FCC) is crucial for converting heavy oil into gasoline and base chemicals in refineries [18,45,6]. During the cracking process, the FCC catalysts continuously accumulate coke and metal contaminants from the feedstock oil (e.g., Ni, Fe, and V) [20,43], called spent catalysts. Metal deposition is detrimental to the activity and selectivity of the catalysts, causing unexpected shifts in product distribution [29]. During the regeneration of the spent catalysts to burn coke, these metal pollutants can also migrate into the flue gas and are discharged into the air as metal particulate matter (PM) [10]. The emissions of metal PM from FCC units are a huge threat to regional ecosystems and human health [5,31].

Due to the adverse effects of metal pollutants on catalyst performance and flue gas emissions, FCC metal poisoning has gradually attracted worldwide attention, coming with heavier and more contaminated crudes in recent years [1,24,39]. It has been proven that metal contaminants can irreversibly block pores and degrade the zeolite, the content of which on FCC spent catalysts ranges from tens to thousands of ppm [14,32,49]. Ni and V, with the highest content, are the most toxic to the fresh catalyst [1,12,13]. The content of Fe is also high, which is not only derived from the feedstock oil but also naturally present in the clay component of the catalysts [17]. Other metal contaminants, such as Cu, Zn, Mn, and so on, are also vital causes of FCC catalyst deactivation [6, 22]. The distribution of these metal contaminants on the spent catalysts usually exhibits a substantial discrepancy [20,22,45]. Previous studies have focused on mapping metal elemental distribution by scanning electron microscopy-energy dispersive spectroscopy (SEM-EDS) and μ-X-Ray fluorescence microscopy (μ-XRF) [17,21,25], which can reveal the metal deposition patterns on the spent catalysts. However, the migration of metal pollutants throughout the FCC process is unclear. The metal-organic compounds in the feedstock oil mostly deposit on the catalysts to form oxides, which may migrate into the air as PM along with the catalyst attrition [33,44,7]. PM in the FCC flue gas contains dozens of trace metal pollutants, mainly Ni, Fe, Cr, and V [5,10]. In particular, relevant studies on the emission of metal PM are rare.

Currently, emission characteristics of FCC metal PM are still poorly understood, although many metal hazardous air pollutants (HAPs) have been listed in some emission inventories of the United States and Europe [15,40]. These inventories have developed the emission factors of FCC flue gas pollutants, excluding metal PM. The emission factors are internationally based on the throughput and coke burning rate of FCC units, which are used to estimate FCC pollutants emissions [9,42]. The lack of metal PM emission factors can be attributed to little data on field monitoring concentrations. U.S. Environmental Protection Agency (EPA) has proposed another approach for FCC metal PM emissions estimates by the default ratio of metal HAP to Ni concentration [42]. Since Ni emission of FCC flue gas has been limited by national regulations [30, 41], the Ni concentration is generally accessible from FCC units. However, the method of ratio factors is less standard and accurate than the emission factors established by directly measured monitoring data of various metal HAPs. Therefore, it is of great practical significance to carry out field monitoring of metal emission concentrations and develop the emission factors of metal PM in FCC units.

In this work, we conducted stack tests of three typical FCC units to monitor the emissions of metal PM in the flue gas. The feedstock oil and spent catalysts collected from the FCC units were characterized by inductively coupled plasma-mass spectrometry (ICP-MS) to measure the content of metal contaminants. According to the monitoring and analysis data, the migration rates of metal pollutants from the feedstock oil to the catalysts to the flue gas were calculated. Besides, the poisoning metal distribution on the spent catalysts was displayed by μ-XRF, which was further used to assess the deposition correlation of different metal elements. Finally, the emission factors of metal PM in the three FCC units were developed based on throughput and coke burning rate. The ratios of metal PM to Ni concentration were also calculated. These results will give further insights into the deposition and emission of FCC metal pollutants, critical for metal poisoning reduction, metal PM emission estimates, and control policy development in the FCC process.

2. Materials and methods

2.1. Sampling sites and methods

Three typical industrial FCC units (U1, U2, and U3) are selected for metal PM sampling, the basic information of which is shown in Table 1. The complete FCC process is displayed in Fig.S1, clearly describing the main structure of the FCC unit. U1 is a 0.8 million tons/year FCC unit, using a full regeneration model with a two-dense phase regenerator. U2 is a 1.4 million tons/year partially regenerated FCC unit with a CO boiler. U3 is a 3.5 million tons/year fully regenerated FCC unit, using rapid bed and turbulent bed series coking process. The three selected FCC units cover the two basic regeneration types (partial regeneration and full regeneration), which can be representative of most FCC regeneration processes in refineries.

According to GB/T 16157–1996 (The determination of particulates and sampling methods of gaseous pollutants from exhaust gas of stationary source) approved by the National Environmental Protection Agency of the People's Republic of China, the sampling site was set at the top of the stack, where the FCC flue gas is discharged into the air. The stack tests should be carried out under normal operating conditions of FCC units. For each unit, three samples of metal PM were collected repeatedly on the stack. Before sampling, the flue gas parameters were measured, including temperature, moisture content, gas composition, pressure, and gas flow rate. The flue gas temperature at the sampling sites is shown in Table S1. The sampling device consisted of an isokinetic nozzle, a filter cartridge, sampling tubes, a condenser, and an air pump. The leak check was conducted after the equipment was connected until the leakage was no more than 0.6 L/min. Then, the sampling nozzle was inserted into the flue, and the air pump was turned on. According to the isokinetic sampling method, the inlet gas speed of the sampling nozzle was adjusted to match the flue gas flow rate. The metal PM in the flue gas was filtered by the filter cartridge, and the gas sampling volume was at least 600 L (dry basis) for each sample. After sampling, the filter cartridge was taken out and sealed for the latter analysis. At the same time, the feedstock oil and catalyst were also collected directly from the three FCC units.

2.2. Sample pretreatment and ICP-MS analysis

The concentrations of metal PM samples were measured according to HJ 777–2015 (Ambient air and waste gas from stationary sources emission -Determination of metal elements in ambient particle matter-Inductively coupled plasma optical emission spectrometry) approved by the Ministry of Environmental Protection of the People's Republic of China. The filter cartridge containing metal PM was cut into small pieces and placed in a digestion tank. 20 mL of aqua regia was slowly added into the tank to immerse the sample. Then, the tank was tightly covered and microwaved for 15 min at 200 ℃. After the filter cartridge was digested, the tank was rinsed with 10 mL of deionized water and held for 30 min at room temperature. The mixed solution in the tank was filtered

Table 1
Basic information of three typical FCC units.

Unit type	Mass flow of feedstock oil (t/h)	Volume flow of flue gas (m^3/h)	Addition of fresh catalysts (t/y)	Removal of spent catalysts (t/y)	Coke burning rate (t/h)
U1	103.07	162,468	900	500	8.96
U2	187.37	130,687	1450	1250	10.52
U3	432.11	424,086	3500	2600	25.06

and diluted to 100 mL for ICP-MS analysis.

ICP-MS analysis was performed by the Inductively Coupled Plasma Atomic Emission Spectrometer (167–785 nm/725) from U.S. Agilent Company, measuring the concentration of 8 kinds of metal elements (Ni, Fe, V, Cr, Mn, Zn, Cu, and As) in the digestion solution. The injection flow rate was 1.0 mL/min and the optical resolution was 0.009 nm. High-purity angon (99.99%) was used as carrier gas with a flow rate of 0.55 mL/min. The detection limit of the main metal elements in the solution was 0.01 mg/L for ICP-MS. After ICP-MS results were obtained, the emission concentration of metal PM in FCC flue gas was calculated by Eq. 1.

$$EC_i = c_i \times Vs/Vg \quad (1)$$

where:

EC_i is the emission concentration of metal PM i, μg/m^3;

c_i is the concentration of metal element i in the digestion solution, μg/mL;

Vs is the volume of the digestion solution, mL;

Vg is the gas sampling volume (dry basis), m^3.

In addition to metal PM samples, feedstock oil and spent catalysts of the three FCC units were also brought back to the laboratory. The samples of spent catalysts were collected in the pipe from the reactor to the regenerator (Fig.S1). 10 g of feedstock oil was weighed and poured into a ceramic crucible. The feedstock oil samples were charred at 300 ℃ for 6 h on an electric heating plate and calcinated at 550 ℃ for 12 h in a Muffle furnace. Then, 10 mL of aqua regia was slowly added into the crucible to dissolve the ash and the solution was diluted with deionized water to 25 mL. Besides, 0.1 g of the spent catalysts was weighed and dissolved using 10 mL aqua regia. The solution was filtered into a volumetric bottle and diluted to 25 mL. These solutions above were also characterized by ICP-MS to measure the content of metal contaminants (Ni, Fe, V, Cr, Mn, Zn, Cu, and As) in the feedstock oil and spent catalysts.

2.3. Calculation of annual amount and migration rate

According to the concentrations of metal pollutants and operating parameters of the three FCC units, the annual amount and migration rate were calculated, as shown in Eq. 2 to Eq. 6. The annual operating time for the three FCC units is 7200 h.

$$At = Co \times Fo \quad (2)$$

$$Ad = Csc \times Fsc - Cfc \times Ffc \quad (3)$$

$$Ae = Cg \times Fg \quad (4)$$

$$Moc = Ad/At \quad (5)$$

$$Mcg = Ae/Ad \quad (6)$$

where:

At is the annual throughput of metal pollutants, t/y;

Ad is the annual deposition of metal pollutants, t/y;

Ae is the annual emission of metal pollutants, t/y;

Co is the concentration of metal pollutants in the feedstock oil, μg/g;

Cfc is the concentration of metal pollutants in the fresh catalysts, μg/g;

Csc is the concentration of metal pollutants in the spent catalysts, μg/g;

Cg is the concentration of metal pollutants in the flue gas, μg/m^3;

Fo is the mass flow of feedstock oil, t/h;

Ffc is the annual addition of the fresh catalysts, t/y;

Fsc is the annual removal of the spent catalysts, t/y;

Fg is the volume flow of flue gas, m^3/h;

Moc is the metal migration rate from the feedstock oil to the catalysts, %;

Mcg is the metal migration rate from the catalysts to the flue gas, %.

2.4. μ-XRF of spent catalysts

Strategies for studying the distribution of metal poisons are to map the FCC catalysts at the single particle level by using synchrotron-based X-ray imaging techniques [18,35,36], such as μ-XRF, μ-X-ray diffraction (μ-XRD), and μ-X-ray absorption near edge spectroscopy (μ-XANES). In this work, μ-XRF analysis was carried out in the Shanghai Synchrotron Radiation Facility BL15U1 beamline station. The spent catalysts were scattered over the detection area and the excess powder was blown away. Under the microscope, the single catalyst particle was selected at the appropriate magnification. A quick XRF analysis was performed to determine the type of metal elements corresponding to each XRF channel. Then, according to the catalyst particle size, a regular square area containing a clear and complete particle was scanned by μ-XRF, using a 1×1 μm^2 beam size. The fluorescence intensity of each point was collected and stored as a matrix. Finally, the images of the spent catalysts were reconstructed using the collected matrix data.

2.5. Calculation of emission factors

The emission factors are actually flue gas pollutant emission rates divided by throughput or coke burning rate according to the international calculation method. Stack tests are one of the primary data sources for emission factors [42]. Accurate measurement of metal PM is critical for emission factor calculation. Two kinds of emission factors were calculated based on the emission concentration of metal PM from the field monitoring in three FCC units. The calculation process of metal PM emission factors is shown in Eq. 7.

$$EF_i = EC_i \times Fg/L \quad (7)$$

where:

EF_i is the emission factor of metal PM i, g/t;

L is the level of device activity, which is represented by the throughput (t/h) or coke burning rate (t/h).

The throughput is the mass flow of feedstock oil, which is directly queried by the online monitoring system of the FCC units. The coke burning rate is generally calculated based on the carbon content of the spent catalysts (Table S2), and the calculation process is shown in Eq. 8. Their values are shown in Table 1.

$$Cbr = Vp \times \rho \times Cc \quad (8)$$

where:

Cbr is the coke burn rate, t/h;

Vp is the air volume (containing spent catalysts) conveyed by circulating inclined pipe from reactor to regenerator, m^3/h;

ρ is the density of the circulating inclined pipe catalysts, kg/m^3;

Cc is the carbon content on the spent catalysts.

2.6. Quality assurance and quality control

During the process of field monitoring, the leak check and flow correction were performed to control system deviation within 5%. The relative deviation between the sampling gas speed and flue gas flow was no more than 10%. At each sampling site of the three FCC units, valid sampling of metal PM was repeated at least three times to improve accuracy and reliability.

Before ICP-MS analysis, the calibration lines of the metal elements were established, and the R^2 value was more than 0.999. After every 15 samples, the calibration lines were determined with the standard solution. When the relative deviation between the measured value and standard value exceeds 10%, the calibration lines should be remade. Blank samples were prepared, including reagent blank and filter

cartridge blank. For reagent blank, the measured value of the target metal element in the chemical regent should be below the detection limit. For the filter cartridge blank, the measured value in the blank sample could not exceed 1/10 of the metal PM concentration. Besides, each sample was measured repeatedly to reduce random errors.

3. Results and discussion

3.1. Metal pollutants in the FCC process

The FCC feedstock oil, mainly including resid, vacuum gas oil (VGO), and heavy gas oil (HGO), contains many trace metal elements and is the primary source of metal contaminations throughout the FCC process [13,32]. These metal substances are gradually incorporated into the catalyst, triggering irreversible deactivation. During the continuous cycle of reaction-regeneration, massive FCC fines from the catalyst attrition are produced and discharged into the atmosphere, causing the emissions of metal PM [3,7]. To figure out the metal characteristics in the three FCC processes, the concentrations of metal pollutants (Ni, Fe, V, Cr, Mn, Zn, Cu, and As) in the feedstock oil, spent catalysts and flue gas were measured, and the results are shown in Fig. 1.

Among the metal contaminations in the feedstock oil, the content of Ni is the highest, with 8.03 ± 0.85, 8.04 ± 1.00, and 5.65 ± 0.54 μg/g for the three units, respectively. Fe and V also perform high concentrations, around 4–5 μg/g. The content of Zn is ten times lower than that of Ni, and the concentrations of the other metal pollutants are much lower than 0.25 μg/g. These metal concentrations are generally consistent with the data from previous literature [6,11]. Compared to crude oil (Table S3), FCC feedstock oil usually has lower metal concentrations due to vacuum distillation treatment. The metal contaminations in the feedstock oil are mainly in the form of metal porphyrin compounds containing Ni, Fe, and V [2,46], which are responsible for the high content of the three metal elements. In Fig. 1(b), the contents of metal elements in the spent catalysts present the same trend as those in the feedstock oil. Ni, Fe, and V are at a high concentration level above 3500 μg/g while the contents of the other metal contaminations are below 300 μg/g. These metal pollutants are hardly detected in the fresh catalysts except Fe (Table S4). The metal deposition is highly correlated with the metal concentration in the feedstock oil [16]. With the coking and burning of the feedstock, the metals in the organic compounds are gradually deposited on the FCC catalysts in the form of oxides [6]. Ni deposition on the catalysts mainly includes NiO and $NiAl_3O_4$ or $NiSiO_3$ [8,37]. NiO can be reduced to Ni^0 in the FCC process, which increases hydrogen and coke yield by promoting dehydrogenation reactions [8,34]. The forms of V are VO_2 and V_2O_5, with high strong polarity and volatility, which easily permeate into the inner layers of the spent catalysts and attack the crystalline structure [39]. Thus, V with high mobility is deposited significantly in the catalysts, and even the concentration of V is more than that of Ni in U1. Fe is in the form of Fe_3O_4, Fe_2O_3, and Fe_2SiO_4, which comes from the feedstock, the matrix, and the equipment corrosion [1,26]. Thus, Fe in the fresh catalysts is also detected (Table S4), with 900, 1200, and 1400 μg/g for the three units. This leads to an additional increase in Fe content on the spent catalyst, as shown in Fig. 1(b), where the concentration of Fe is higher than that of

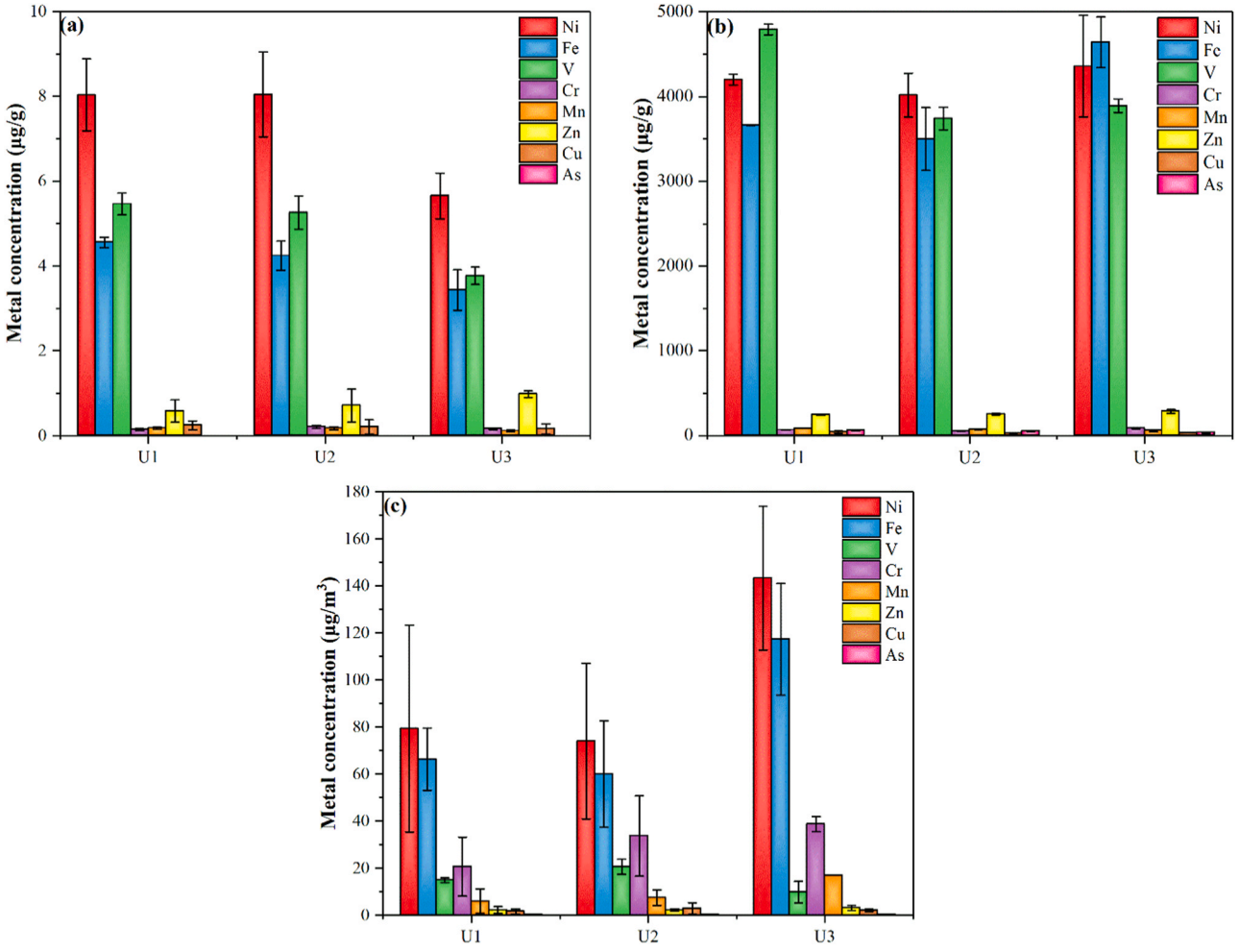

Fig. 1. The concentration of metal pollutants. (a) in feedstock oil. (b) in spent catalysts. (c) in flue gas.

Ni in U3. These metal oxides can rarely be removed by coke burning and continuously accumulate on the catalysts. During the regeneration process, these metal pollutants enter the flue gas in the form of fine particles, and the concentration of metal PM is shown in Fig. 1(c).

The emission concentrations of Ni and Fe are the highest, around 80–140 μg/m^3, which are consistent with the content in the feedstock and spent catalysts. Except this, other metal pollutants exhibit different trends. The emission concentration of V is 10–20 μg/m^3 while Cr has a relatively high concentration of 20–40 μg/m^3. The unexpected emission characteristics of V and Cr are consistent with the monitoring data in previous studies, as shown in Table S3. This might be related to the distribution of metal contaminants on the catalysts, and those in the outer layer of the catalyst particles are more easily worn into the flue gas. For Mn, Zn, Cu, and As, the emission concentrations are much lower than 20 μg/m^3. Besides, the emission concentrations of Ni and Fe in U1 and U3 are significantly higher than those in U2, which is attributed to different regeneration processes. Currently, Ni in the metal PM is the focus of the refinery. For FCC units, the emission of Ni PM is limited to 0.5 mg/m^3 in China and 1 mg/1000 coke burn-off in the United States [30,41]. Other metal pollutants have not been regulated. Rising environmental requirements will push these metal pollutants into new emission standards, and emission limits should be reformulated. This study on the emission characteristics of metal PM can provide data reference for future FCC emissions regulations.

3.2. Migration of metal pollutants

Understanding the migration of metal pollutants is essential to mitigate metal poisons and control metal emissions in the FCC process. Compared with analyzing metal concentrations, calculating the metal migration rates by the annual amount of metal contaminants in the three processes is more suitable for studying metal migration, as it can reflect the operating level of different FCC units and reveal the metal migration patterns. Here, the annual throughput, deposition, and emission of metal pollutants throughout the FCC process were calculated, as shown in Table 2, and their migration rates are present in Table 3. A diagram of metal migration can be seen in Fig.S2.

Due to the high concentration of metal contaminants in the feed, the annual metal throughput exceeds 10, 20, and 40 t/y for U1, U2, and U3. The risk of metal poisoning calls for improved metal tolerance and increased catalyst usage. The FCC metal passivators have been widely used to combat metal poisons [8,34]. Internationally, converting a barrel of feedstock requires 0.16 kg of FCC catalysts (about 0.35 lbs per bbl) [45]. In the three FCC units, the catalysts required by the feedstock oil are 0.16, 0.15, and 0.15 kg per bbl. From the feedstock oil to the catalysts, the metal deposition is notable, and the migration rates of Ni, Fe, and V reach 30–90%. In the porphyrin complexes of these three metal contaminants, pyrrolic nitrogen (N-5) with basicity can easily interact with acid sites on the catalysts [23,38]. Thus, Ni, Fe, and V are more inclined to deposit and have higher migration rates than the other metals (10–45%).

Obviously, in the FCC process, the metal contaminants in the feedstock oil mainly migrate to the catalysts. The metal deposition amount is astonishing, especially the most deleterious Ni and V, exceeding 10 t/y in U3. To maintain the overall catalytic activity in FCC units, a small portion of the spent catalysts are continuously removed and replaced by fresh catalysts [3,7]. The high metal accumulation poses a challenge to the disposal of the FCC spent catalysts, which have been classified as hazardous waste in the “European Solid Waste/Hazardous Waste List” (waste number 160804) and “National Hazardous Waste List” (waste code 251–117–50) [4,47]. The heavy metals on the spent catalysts after disposal gradually penetrate into soil and water, which can endanger aquatic ecosystems and human health [19,28]. During the catalyst regeneration process, the migration trend differs from metal deposition’s. From the spent catalysts to the flue gas, the mobility of Cr and Mn is particularly high, the former above 45% and the latter around 7–35%. The migration rates of Ni, Fe, and Cu range from 1% to 10% while those of V, Zn, and As are below 2.5%. The migration process of metal emissions is mainly caused by catalyst attrition. The location of the metal contaminants on the catalysts is critical for mobility. Metals in the outer layers of the catalysts are easier to enter the flue gas, showing high migration rates. Those in the inner region are less likely to migrate, particularly V with high concentration and low migration rate. Besides, the metal migration rates in fully regenerated U1 and U3 are generally greater than those in partially regenerated U2, indicating that the regeneration process is also a vital factor affecting metal pollutants’ entry into the flue gas. In addition, considering the treatment system of FCC flue gas (Fig.S1), the mass of FCC fines from the catalyst attrition is more than emissions in the flue gas. Thus, the metal mobility from the catalyst to the flue gas is actually higher. Although the emission concentrations of these metal pollutants are not high and well within the limits, the metal annual emissions are still considerable due to the large flue gas flow of the FCC units. The emissions of regulated Ni PM in the three units are 93, 70, and 420 kg/y, respectively. The total annual emissions of metal pollutants are over 220, 180, and 940 kg/y for U1, U2, and U3, respectively. The metal PM should be monitored and controlled because of its high toxicity and ecological pollution.

3.3. Metal distribution on the spent catalysts

Defining the metal distribution on the spent catalysts is critical to deeply elucidate metal migration in the FCC process. The study on the content of metal contaminants cannot reveal their deposition and distribution. μ-XRF, a powerful imaging technology, has been applied to image poisoning metals distribution with high spatial resolution in a non-invasive fashion [45]. Here, μ-XRF was utilized to characterize the single particle of the spent catalysts (Cat_1, Cat_2, and Cat_3) in three FCC units with the 1 μm spatial resolution, and the 2-D distribution of metal poisons is shown in Fig. 2.

It can be immediately observed that the hotspot regions appear in the maps of Fe, Ni, and V, indicating the inhomogeneity of metal deposition at the high-concentration level [17]. The average information at the macro scale will present spatial heterogeneities at the single particle level [48], which can also be served in the microscope pictures of the spent catalysts in Fig.S3. Ni is concentrated on the surface of the catalyst particles while V deposits deeper into the interior region, which is in line

Table 2
Annual amount of metal pollutants from feedstock oil, catalysts, and flue gas (t/y).

Samples	Units	Ni	Fe	V	Cr	Mn	Zn	Cu	As
Feedstock oil	U1	5.96	3.38	4.05	0.11	0.13	0.43	0.18	-
	U2	10.85	5.72	7.09	0.28	0.24	0.96	0.28	-
	U3	17.58	10.67	11.72	0.51	0.35	3.04	0.48	-
Spent catalysts	U1	2.10	1.02	2.40	0.032	0.041	0.11	0.021	0.030
	U2	5.02	2.63	4.67	0.066	0.092	0.29	0.034	0.066
	U3	11.33	7.17	10.12	0.22	0.15	0.69	0.073	0.096
Flue gas	U1	0.093	0.078	0.018	0.024	0.0070	0.0027	0.0019	0.00030
	U2	0.070	0.056	0.019	0.032	0.0070	0.0021	0.0027	0.00027
	U3	0.42	0.34	0.029	0.11	0.049	0.0092	0.0060	0.00096

Table 3
Migration rate of metal pollutants from feedstock oil to spent catalysts to flue gas (%).

Samples	Units	Ni	Fe	V	Cr	Mn	Zn	Cu	As
Feedstock oil to spent catalysts	U1	35.23	30.18	59.26	29.09	31.54	25.58	11.67	-
	U2	46.27	45.98	65.87	23.57	38.33	30.21	12.14	-
	U3	64.45	67.20	86.35	43.14	42.86	22.70	15.21	-
Spent catalysts to flue gas	U1	4.43	7.65	0.75	75.00	17.07	2.45	9.05	1.00
	U2	1.39	2.13	0.41	48.48	7.61	0.72	7.94	0.41
	U3	3.71	4.74	0.29	50.00	32.67	1.33	8.22	1.00

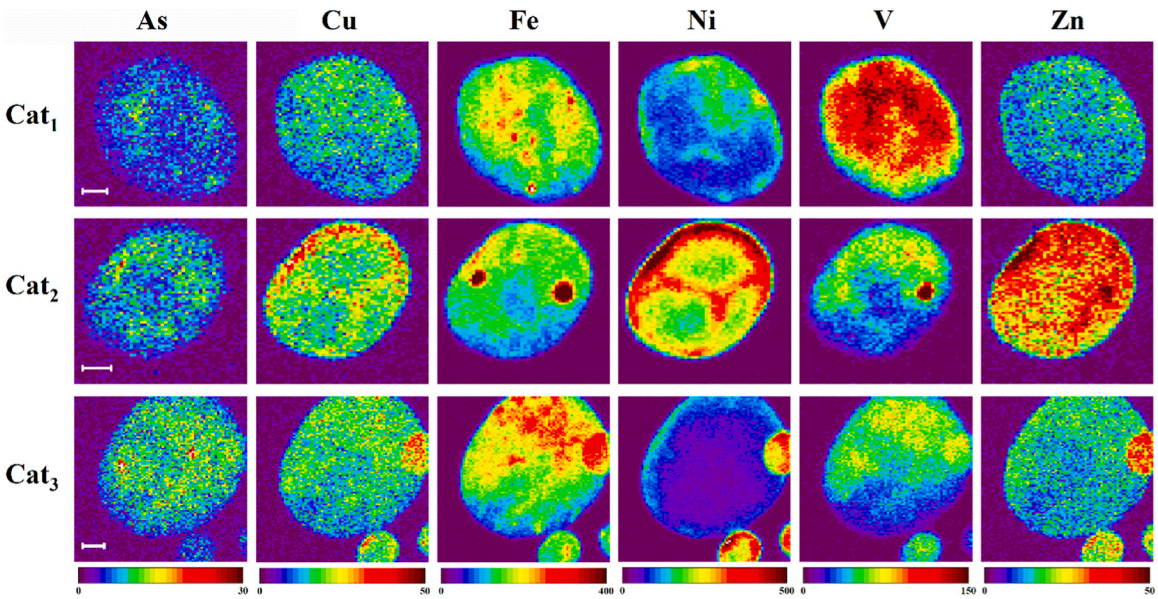

Fig. 2. Elemental distribution maps of metal contaminants on three spent catalysts, obtained after batch fitting analysis of the μ-XRF dataset. The intensity limits for each element are set to the same values for three spent catalysts. The scale bar (white) indicates 10 μm.

with previous studies [22,36]. This distribution phenomenon elucidates the difference between Ni and V emissions in FCC flue gas. Regarding Fe, the spent catalyst presents a Fe-rich distribution through the whole particle with a higher concentration in the inner part. Fe is naturally contained in the catalyst matrix, but it is also deposited from the feedstock oil and steel corrosion in the unit [1,17]. The Fe XRF map for the fresh catalyst is shown in Fig.S4, indicating that Fe is distributed in the middle region of the particle. The Fe distribution on the fresh and spent catalysts shows that Fe tends to deposit from the feedstock oil to the outer layer of the catalysts [21]. As for other metal contaminants, Cu is preferentially in the near-surface regions of the catalyst particle, while Zn mainly penetrates into the deeper part, and As is lightly distributed throughout the catalyst particle. Cr and Mn were not recognized in the μ-XRF experiments, and their distribution cannot be displayed. Based on the metal migration rates from the catalyst to the flue gas, Cr and Mn are likely to be located in the outer layer of the catalysts. Obviously, the metal distribution can be divided into two categories: egg-shell and egg-yolk. The metal deposition in the outer layers clogs the macropores to restrict feedstock molecule access to active domains while the metal accumulation in the inner layers gradually destroys the zeolite framework, causing the irreversible deactivation of the FCC catalysts [36].

To further understand metal poisons, we calculated the distribution correlation of metal elements using matrix intensity data measured by μ-XRF through correlation analysis. The calculation results of Pearson Correlation Coefficients (PCC) are shown in Fig. 3. For the three spent catalysts, the correlation trends between metal elements are similar, suggesting the regularity of metal deposition in the FCC process. Ni and Cu are highly correlated, especially in the near-surface region of the particle (Fig. 2), where they gather together to form a metal shell that severely limits access to the catalyst particle [22]. The V-Fe PCC is much high, notably correlated inside the catalyst particle. Considering the distribution of Fe in the fresh catalysts, the V-Fe PCC hints that V penetrates deeper into the particle and is present in the matrix component of the FCC catalyst. Generally, the study on metal distribution and correlation sheds new insight into the metal poisons on the FCC catalyst, which will upgrade the protocols for artificially mimicking the aging of the FCC catalysts in the laboratory to reveal the deactivation mechanism. Furthermore, this work will help develop strategies to mitigate metal deposition and restore the activity of poisoned catalysts.

3.4. Emission factors of FCC metal PM

The emission factors are an essential method to estimate and predict gas pollutant emissions, especially when a continuous emission monitoring system (CEMS) is not equipped and field monitoring data cannot be provided. Currently, the monitoring of metal PM in FCC units is challenging under field conditions. In this work, the emission concentrations of metal PM in the FCC flue gas have been obtained by field monitoring. Here, according to the monitoring results of stack tests, we have developed two emission factors (based on throughput and coke burning rate) of FCC metal pollutants, which are shown in Fig. 4.

The throughput and coke burning rate are highly correlated with the emissions of FCC flue gas pollutants, the former more readily available and the latter more relevant [27]. Similar trends are observed for the two emission factors based on them, indicating little change in feed and operating conditions in the three FCC units. In this case, the emission factors based on throughput are a more convenient option, while the other emission factors are preferred as the conditions change significantly. As for the eight metal PMs, the values of emission factors present discrepancies, which are directly related to the emission concentration

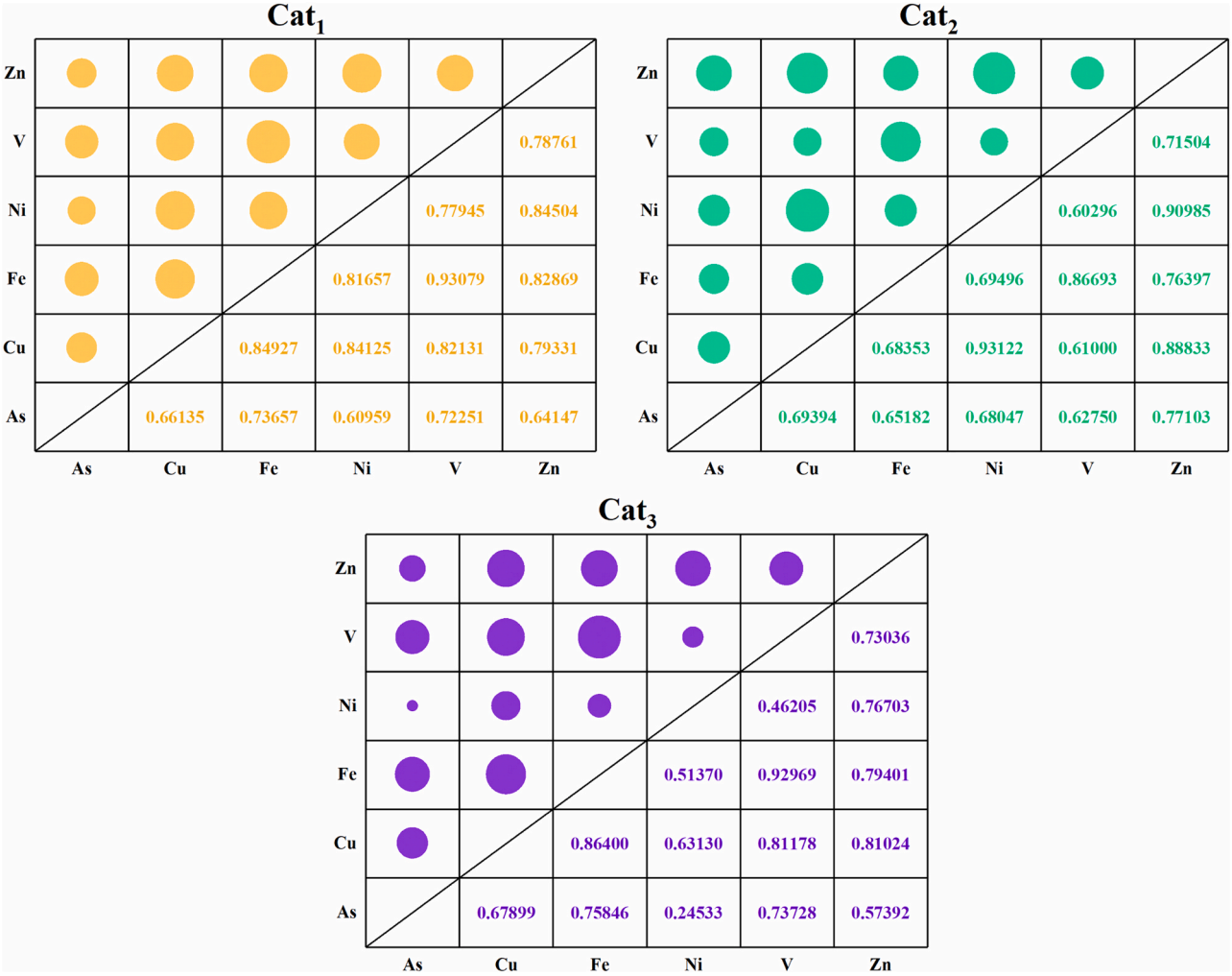

Fig. 3. Pearson Correlation Coefficients (PCC) of metal distribution for three spent catalysts.

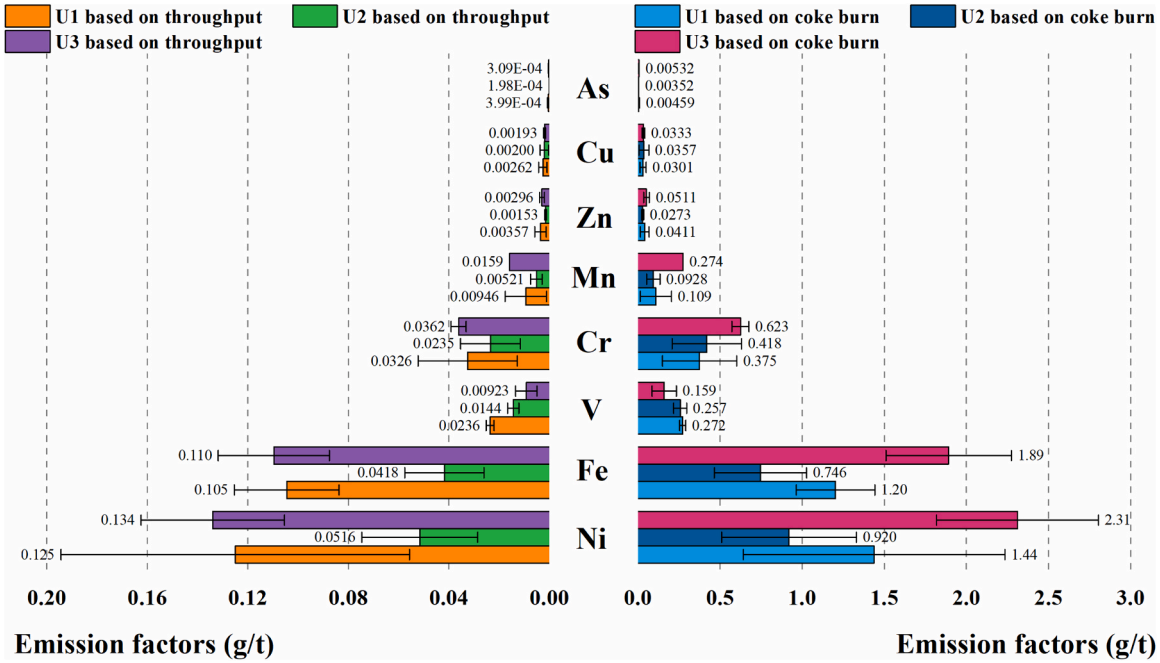

Fig. 4. Two emission factors for metal PM. Based on throughput (left) and coke burning rate (right).

in FCC flue gas. Ni and Fe have the highest emission factors, followed by V, Cr, Mn, and Zn. The emission factors of Cu and As are much lower, below 0.005 g/t (based on throughput) or 0.05 g/t (based on coke burning rate). The results are fundamentally attributed to the difference in metal contaminants deposition. The contaminants in the form of oxides on the spent catalysts don't decompose during regeneration and are emitted into the flue gas along with the catalyst attrition. The content and distribution of metal elements on the spent catalysts determine the likelihood of entering the flue gas. Therefore, despite similarly high content on the spent catalysts, Ni on the exterior has much higher emission factors than V in the deeper layer.

Besides, the regeneration process is another vital influence factor. The emission factors of metal PM vary enormously from unit to unit. Generally, the emission factors in the full regeneration unit (U1 and U3) are higher than those in the partial regeneration unit (U2). Higher oxygen content and temperature could increase catalyst attrition during regeneration, leading to more FCC fines. The monitoring results of PM in the three FCC units have confirmed the assumption. The emission concentrations of PM are 102.70 mg/m^3 (U1), 41.1 mg/m^3 (U2), and 100.57 mg/m^3 (U3). In general, the emission factors of metal PM are much lower than those of common FCC flue gas pollutants provided by the US EPA [40], such as 235 g/t for NO_x and 1630 g/t for SO_2 (based on throughput). Nevertheless, considering the large amount of feedstock and flue gas emissions in FCC units, the metal PM emissions obtained by emission factor estimation should be paid more attention.

Unexpectedly, the US EPA and European Environment Agency (EEA) haven't developed the emission factors of metal PM for FCC units. Instead, EPA has established an equivalent means based on the ratio of metal pollutants to Ni concentration, and the detailed data is displayed in Table S5. Here, we call this method the ratio factor. According to the EPA method, the ratio factors of metal PM for the three FCC units were calculated, as shown in Fig. 5(a). Compared with EPA data, the three FCC units in China exhibit a substantial deviation. Especially the EPA ratio factors of V and Zn are much higher than those in the study. The main reason for the gap is the feedstock of FCC units from different countries and areas, with significant differences in metal contaminant content [16,6,7]. To further analyze the discrepancy, the EPA ratio factors are used to estimate the emissions of metal PM from the three FCC units. The relative errors between the estimated value and the field monitoring results are shown in Fig. 5(b), where a gargantuan deviation is observed. The relative errors of Zn even reach 2490.00%, 2389.09%, and 3249.47%, and that of V in U3 is 1817.56%. The emissions of As, Zn, and V are severely overestimated while the emission of Cr is underestimated. Obviously, the EPA ratio factors are unsuitable for evaluating the metal PM emissions from the FCC units in China. The ratio factors provided in this study have improved the estimation reliability of site-specific emissions of FCC metal PM.

Considering that the emission concentration of Ni has been monitored in the refinery, the ratio factor is quite convenient for the emission estimation of metal PM. However, according to the international inventories, the emission factor is always a more standard and accurate assessment method. The ratio factor can be used instead in the absence of relevant data. Therefore, the establishment of FCC metal PM emission factors in this work has filled the data gap and promoted the accuracy of emission estimation, which will further support the development of emission inventory for FCC units.

4. Conclusion

In this work, the metal PM in the flue gas was collected through the stack tests of the three FCC units. Together with the feedstock oil and the spent catalysts, the metal PM samples were analyzed for the metal concentrations. The concentrations of Ni and Fe are the highest in all three phases, while V with a high concentration in the feedstock oil and spent catalysts behaves inconsistently in the flue gas. In the deposition process, Ni, Fe, and V present higher migration rates than Cr, Mn, Zn, Cu, and As. However, from the catalysts to the flue gas, the migration rates of Cr and Mn are the highest, followed by Cu, Ni, and Fe. The mobility of Zn, As, and V is much lower. The differences in migration and emission are attributed to the metal distribution on the spent catalysts and regeneration process.

μ-XRF measurements indicate that Ni and Cu are concentrated on the exterior of the catalysts while V and Zn penetrate into the particles' deeper layers. The high correlation between V and Fe indicates that V is mainly deposited in the matrix region of the catalysts. The distribution of metal deposition is in line with the metal emission concentration in FCC flue gas. Based on the field monitoring results, the metal PM emission factors were established, ranging from 0.0002 to 0.02 g/t based on throughput and 0.003–3.0 g/t based on coke burning rate. The ratio factors for the three FCC units were also calculated, and a gargantuan discrepancy was found compared to EPA data, showing the inapplicability of EPA ratio factors. Therefore, the development of emission factors has complemented the research lack and improved the accuracy of metal PM estimation. With the increased environmental issues, the FCC metal pollutants are bound to be the focus in refineries. The study on metal migration and emission can be the theoretical basis for emission control and estimation of the FCC metal pollutants.

Environmental Implication

Metal pollutants with high toxicity are detrimental to local ecosystems and human health, such as the itai-itai disease caused by Cd. In the fluid catalytic cracking (FCC) unit, the metal pollutants in feedstock poison the catalysts, referring to spent catalysts. A portion of the spent

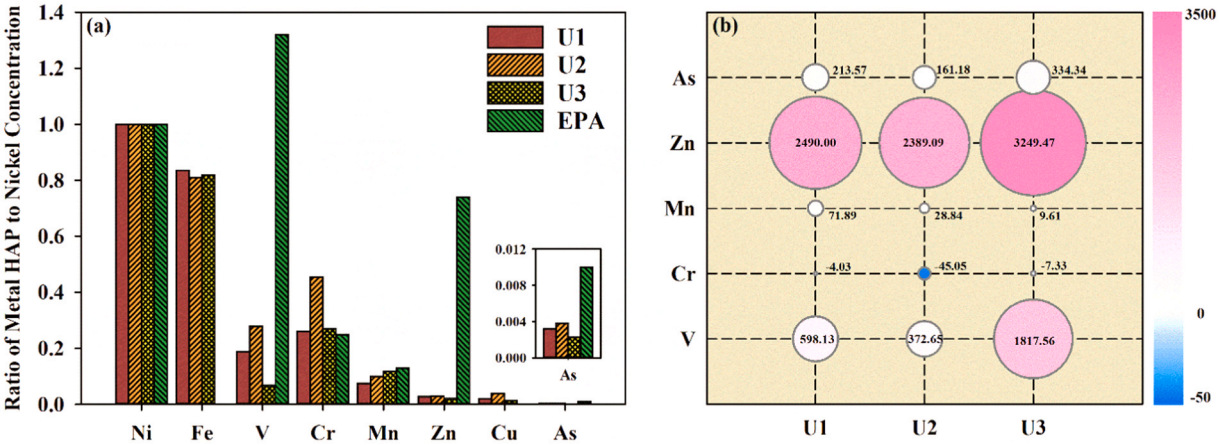

Fig. 5. Comparison of ratio factors for metal PM. (a) Ratio factors. (b) Relative errors (%).

catalysts are treated by landfills, causing metal pollution of groundwater. The others are regenerated, resulting in massive metal particulate matter (PM) being emitted into the air. This study helps understand the migration and emission of metal pollutants, which will shed new insight into metal poisoning mitigation and metal PM emission control in FCC units.

CRediT authorship contribution statement

Jiawei Bian: Conceptualization, Methodology, Writing – original draft, Visualization. **Bohan Wang:** Investigation, Data curation. **Ximing Niu:** Validation. **Hai Zhao:** Formal analysis. **Hao Ling:** Supervision, Funding acquisition. **Feng Ju:** Writing – review & editing, Project administration.

Declaration of Competing Interest

The authors declare that they have no known competing financial interests or personal relationships that could have appeared to influence the work reported in this paper.

Data Availability

Data will be made available on request.

Acknowledgements

This work was supported by the National Natural Science Foundation of China (22378131).

Appendix A. Supporting information

Supplementary data associated with this article can be found in the online version at doi:10.1016/j.jhazmat.2023.132778.

References

[1] Adanenche, D.E., Aliyu, A., Atta, A.Y., El-Yakubu, B.J., 2023. Residue fluid catalytic cracking: a review on the mitigation strategies of metal poisoning of RFCC catalyst using metal passivators/traps. Fuel 343, 127894. https://doi.org/10.1016/j.fuel.2023.127894.

[2] Ali, M.F., Abbas, S., 2006. A review of methods for the demetallization of residual fuel oils. Fuel Process Technol 87 (7), 573–584. https://doi.org/10.1016/j.fuproc.2006.03.001.

[3] Almas, Q., Naeem, M.A., Baldanza, M.A.S., Solomon, J., Kenvin, J.C., Müller, C.R., Teixeira da Silva, V., Jones, C.W., Sievers, C., 2019. Transformations of FCC catalysts and carbonaceous deposits during repeated reaction-regeneration cycles. Catal Sci Technol 9 (24), 6977–6992. https://doi.org/10.1039/c9cy01680e.

[4] Alonso-Farinas, B., Rodriguez-Galan, M., Arenas, C., Arroyo Torralvo, F., Leiva, C., 2020. Sustainable management of spent fluid catalytic cracking catalyst from a circular economy approach. Waste Manag 110, 10–19. https://doi.org/10.1016/j.wasman.2020.04.046.

[5] Amoatey, P., Omidvarborna, H., Baawain, M.S., Al-Mamun, A., 2019. Emissions and exposure assessments of SO_X, NO_X, $PM_{10/2.5}$ and trace metals from oil industries: a review study (2000–2018). Process Saf Environ Prot 123, 215–228. https://doi.org/10.1016/j.psep.2019.01.014.

[6] Bai, P., Etim, U.J., Yan, Z., Mintova, S., Zhang, Z., Zhong, Z., Gao, X., 2018. Fluid catalytic cracking technology: current status and recent discoveries on catalyst contamination. Catal Rev -Sci Eng 61 (3), 333–405. https://doi.org/10.1080/01614940.2018.1549011.

[7] Cerqueira, H.S., Caeiro, G., Costa, L., Ramôa Ribeiro, F., 2008. Deactivation of FCC catalysts. J Mol Catal A-Chem 292 (1–2), 1–13. https://doi.org/10.1016/j.molcata.2008.06.014.

[8] Charisteidis, I.D., Trikalitis, P.N., Triantafyllidis, K.S., Komvokis, V., Yilmaz, B., 2022. Characterization of Ni-phases and their transformations in fluid catalytic cracking (FCC) catalysts: comparison of conventional versus boron-based Ni-passivation. Catalysts 13 (1), 3. https://doi.org/10.3390/catal13010003.

[9] CONCAWE, 2019. Air pollutant emission estimation methods for E-PRTR reporting by refineries, 2019 edition. ⟨https://www.concawe.eu/wp-content/uploads/Rpt_19–4.pdf⟩.

[10] de la Campa, A.M., Moreno, T., de la Rosa, J., Alastuey, A., Querol, X., 2011. Size distribution and chemical composition of metalliferous stack emissions in the San Roque petroleum refinery complex, Southern Spain. J Hazard Mater 190 (1–3), 713–722. https://doi.org/10.1016/j.jhazmat.2011.03.104.

[11] Doyle, A., Saavedra, A., Tristão, M.L.B., Aucelio, R.Q., 2015. Determination of S, Ca, Fe, Ni and V in crude oil by energy dispersive X-ray fluorescence spectrometry using direct sampling on paper substrate. Fuel 162, 39–46. https://doi.org/10.1016/j.fuel.2015.08.072.

[12] Etim, U.J., Bai, P., Liu, X., Subhan, F., Ullah, R., Yan, Z., 2019. Vanadium and nickel deposition on FCC catalyst: Influence of residual catalyst acidity on catalytic products. Microporous Mesoporous Mater 273, 276–285. https://doi.org/10.1016/j.micromeso.2018.07.011.

[13] Etim, U.J., Xu, B., Bai, P., Ullah, R., Subhan, F., Yan, Z., 2016. Role of nickel on vanadium poisoned FCC catalyst: a study of physiochemical properties. J Energy Chem 25 (4), 667–676. https://doi.org/10.1016/j.jechem.2016.04.001.

[14] Etim, U.J., Xu, B., Ullah, R., Yan, Z., 2016. Effect of vanadium contamination on the framework and micropore structure of ultra stable Y-zeolite. J Colloid Interface Sci 463, 188–198. https://doi.org/10.1016/j.jcis.2015.10.049.

[15] European Environment Agency (EEA), 2019. EMEP/EEA air pollutant emission inventory guidebook 2019. ⟨https://www.eea.europa.eu/publications/emep-eea-guidebook-2019⟩.

[16] Fu, H., Chen, Y., Liu, T., Zhu, X., Yang, Y., Song, H., 2021. Research on hazardous waste removal management: identification of the hazardous characteristics of fluid catalytic cracking spent catalysts. Molecules 26 (8), 2289. https://doi.org/10.3390/molecules26082289.

[17] Gambino, M., Nieuwelink, A.E., Reints, F., Veselý, M., Filez, M., Ferreira Sanchez, D., Grolimund, D., Nesterenko, N., Minoux, D., Meirer, F., Weckhuysen, B.M., 2021. Mimicking industrial aging in fluid catalytic cracking: a correlative microscopy approach to unravel inter-particle heterogeneities. J Catal 404, 634–646. https://doi.org/10.1016/j.jcat.2021.10.012.

[18] Gambino, M., Vesely, M., Filez, M., Oord, R., Ferreira Sanchez, D., Grolimund, D., Nesterenko, N., Minoux, D., Maquet, M., Meirer, F., Weckhuysen, B.M., 2020. Nickel poisoning of a cracking catalyst unravelled by single-particle X-ray fluorescence-diffraction-absorption tomography. Angew Chem -Int Ed 59 (10), 3922–3927. https://doi.org/10.1002/anie.201914950.

[19] Hassanzadeh-Afruzi, F., Esmailzadeh, F., Asgharnasl, S., Ganjali, F., Taheri-Ledari, R., Maleki, A., 2022. Efficient removal of Pb(II)/Cu(II) from aqueous samples by a guanidine-functionalized SBA-15/Fe_3O_4. Sep Purif Technol 291. https://doi.org/10.1016/j.seppur.2022.120956.

[20] Ihli, J., Jacob, R.R., Holler, M., Guizar-Sicairos, M., Diaz, A., da Silva, J.C., Ferreira Sanchez, D., Krumeich, F., Grolimund, D., Taddei, M., Cheng, W., Shu, Y., Menzel, A., van Bokhoven, J.A., 2017. A three-dimensional view of structural changes caused by deactivation of fluid catalytic cracking catalysts. Nat Commun 8 (1), 809. https://doi.org/10.1038/s41467-017-00789-w.

[21] Jiang, H., Livi, K.J., Kundu, S., Cheng, W.-C., 2018. Characterization of iron contamination on equilibrium fluid catalytic cracking catalyst particles. J Catal 361, 126–134. https://doi.org/10.1016/j.jcat.2018.02.025.

[22] Kalirai, S., Boesenberg, U., Falkenberg, G., Meirer, F., Weckhuysen, B.M., 2015. X-ray fluorescence tomography of aged fluid-catalytic-cracking catalyst particles reveals insight into metal deposition processes. ChemCatChem 7 (22), 3674–3682. https://doi.org/10.1002/cctc.201500710.

[23] Li, S., Jiang, Q., Qi, Y., Zhao, D., Tang, Y., Liu, Q., Chen, Z., Zhu, Y., Dai, B., Song, H., Zhang, L., 2022. Influence of coke heterogeneity and the interaction between different coke species on the emission of toxic HCN and NO(x) from FCC spent catalyst regeneration. J Hazard Mater 436, 129187. https://doi.org/10.1016/j.jhazmat.2022.129187.

[24] Liao, Y., Liu, T., Du, X., Gao, X., 2021. Distribution of iron on FCC catalyst and its effect on catalyst performance. Front Chem 9, 640413. https://doi.org/10.3389/fchem.2021.640413.

[25] Liao, Y., Liu, T., Zhao, H., Gao, X., 2021. A comparison of laboratory simulation methods of iron contamination for FCC catalysts. Catalysts 11 (1), 104. https://doi.org/10.3390/catal11010104.

[26] Liu, Q., Peng, B., Zhou, Q., Zheng, A., Gao, X., Qi, Y., Yuan, S., Zhu, Y., Zhang, L., Song, H., Da, Z., 2022. Role of iron contaminants in the pathway of ultra-stable Y zeolite degradation. Catal Sci Technol 12 (13), 4145–4156. https://doi.org/10.1039/d2cy00672c.

[27] Luan, H., Wu, C., Xiu, G., Ju, F., Ling, H., Pan, H., 2022. Study on emission factors of FCC flue gas pollutants in petroleum refineries. Environ Sci Pollut Res 29 (22), 33400–33410. https://doi.org/10.1007/s11356-021-16767-1.

[28] Maleki, A., Hajizadeh, Z., Sharifi, V., Emdadi, Z., 2019. A green, porous and eco-friendly magnetic geopolymer adsorbent for heavy metals removal from aqueous solutions. J Clean Prod 215, 1233–1245. https://doi.org/10.1016/j.jclepro.2019.01.084.

[29] Meirer, F., Kalirai, S., Morris, D., Soparawalla, S., Liu, Y., Mesu, G., Andrews, J.C., Weckhuysen, B.M., 2015. Life and death of a single catalytic cracking particle. Sci Adv 1 (3), e1400199. https://doi.org/10.1126/sciadv.1400199.

[30] MEPC Emission standard of pollutants for petroleum refining industry; 2015.

[31] Moreno, T., Querol, X., Alastuey, A., de la Rosa, J., Sanchez de la Campa, A.M., Minguillon, M., Pandolfi, M., Gonzalez-Castanedo, Y., Monfort, E., Gibbons, W., 2010. Variations in vanadium, nickel and lanthanoid element concentrations in urban air. Sci Total Environ 408 (20), 4569–4579. https://doi.org/10.1016/j.scitotenv.2010.06.016.

[32] Nazarova, G., Ivashkina, E., Ivanchina, E., Oreshina, A., Dolganova, I., Pasyukova, M., 2020. Modeling of the catalytic cracking: catalyst deactivation by coke and heavy metals. Fuel Process Technol 200. https://doi.org/10.1016/j.fuproc.2019.106318.

[33] Psarras, A.C., Iliopoulou, E.F., Kostaras, K., Lappas, A.A., Pouwels, C., 2009. Investigation of advanced laboratory deactivation techniques of FCC catalysts via FTIR acidity studies. Microporous Mesoporous Mater 120 (1–2), 141–146. https://doi.org/10.1016/j.micromeso.2008.09.014.

[34] Qi, Y., Liu, Q., Chen, Z., Zhu, Y., Chen, Y., Song, H., Dai, B., Zhang, L., 2023. Nickel-passivating element selection in FCC process and mechanistic study on the passivation of nickel by lanthanum and phosphorus. Chem Eng J 467, 143452. https://doi.org/10.1016/j.cej.2023.143452.

[35] Qi, Y., Liu, Q., Li, S., Zhou, Q., Chen, Z., Zhu, Y., Chen, Y., Song, H., Lu, Y.R., Chan, T.S., Dai, B., Zhang, L., 2022. Quantitative determination of nickel speciation for the presence of free oxide in commercial fluid catalytic cracking catalysts. Fuel Process Technol 230, 107207. https://doi.org/10.1016/j.fuproc.2022.107207.

[36] Ruiz-Martinez, J., Beale, A.M., Deka, U., O'Brien, M.G., Quinn, P.D., Mosselmans, J.F., Weckhuysen, B.M., 2013. Correlating metal poisoning with zeolite deactivation in an individual catalyst particle by chemical and phase-sensitive X-ray microscopy. Angew Chem -Int Ed 52 (23), 5983–5987. https://doi.org/10.1002/anie.201210030.

[37] Senter, C., Mastry, M.C., Zhang, C.C., Maximuck, W.J., Gladysz, J.A., Yilmaz, B., 2021. Role of chlorides in reactivation of contaminant nickel on fluid catalytic cracking (FCC) catalysts. Appl Catal A-Gen 611, 117978. https://doi.org/10.1016/j.apcata.2020.117978.

[38] Shi, J., Guan, J., Guo, D., Zhang, J., France, L.J., Wang, L., Li, X., 2016. Nitrogen chemistry and coke transformation of FCC coked catalyst during the regeneration process. Sci Rep 6 (1), 27309. https://doi.org/10.1038/srep27309.

[39] Souza, N.L.A., Tkach, I., Morgado, E., Krambrock, K., 2018. Vanadium poisoning of FCC catalysts: a quantitative analysis of impregnated and real equilibrium catalysts. Appl Catal A-Gen 560, 206–214. https://doi.org/10.1016/j.apcata.2018.05.003.

[40] U.S. EPA, 1995. AP-42: Compilation of Air Emissions Factors. ⟨https://www.epa.gov/air-emissions-factors-and-quantification/ap-42-compilation-air-emissions-factors⟩.

[41] U.S. EPA, 2013. Petroleum Refineries: National Emission Standards for Hazardous Air Pollutants (NESHAP). ⟨https://www.epa.gov/stationary-sources-air-pollution/petroleum-refineries-national-emission-standards-hazardous-air⟩.

[42] U.S. EPA, 2015. Emissions Estimation Protocol for Petroleum Refineries-Version 3.0. ⟨https://www.epa.gov/air-emissions-factors-and-quantification/emissions-estimation-protocol-petroleum-refineries⟩.

[43] Veselý, M., Valadian, R., Lohse, L.M., Toepperwien, M., Spiers, K., Garrevoet, J., Vogt, E.T.C., Salditt, T., Weckhuysen, B.M., Meirer, F., 2021. 3–D X-ray nanotomography reveals different carbon deposition mechanisms in a single catalyst particle. ChemCatChem 13 (10), 2494–2507. https://doi.org/10.1002/cctc.202100276.

[44] Vincz, C., Rath, R., Smith, G.M., Yilmaz, B., McGuire, R., 2015. Dendritic nickel porphyrin for mimicking deposition of contaminant nickel on FCC catalysts. Appl Catal A-Gen 495, 39–44. https://doi.org/10.1016/j.apcata.2015.01.043.

[45] Vogt, E.T., Weckhuysen, B.M., 2015. Fluid catalytic cracking: recent developments on the grand old lady of zeolite catalysis. Chem Soc Rev 44 (20), 7342–7370. https://doi.org/10.1039/c5cs00376h.

[46] Vogt, E.T.C., Fu, D., Weckhuysen, B.M., 2023. Carbon deposit analysis in catalyst deactivation, regeneration, and rejuvenation. Angew Chem -Int Ed 62 (29), e202300319. https://doi.org/10.1002/anie.202300319.

[47] Wang, Y.J., Wang, C., Li, L.L., Chen, Y., He, C.H., Zheng, L., 2021. Assessment of ecotoxicity of spent fluid catalytic cracking (FCC) refinery catalysts on Raphidocelis subcapitata and predictive models for toxicity. Ecotox Environ Safe 222, 112466. https://doi.org/10.1016/j.ecoenv.2021.112466.

[48] Weckhuysen, B.M., 2009. Chemical imaging of spatial heterogeneities in catalytic solids at different length and time scales. Angew Chem -Int Ed 48 (27), 4910–4943. https://doi.org/10.1002/anie.200900339.

[49] Xie, Y., Zhang, Y., He, L., Jia, C.Q., Yao, Q., Sun, M., Ma, X., 2023. Anti-deactivation of zeolite catalysts for residue fluid catalytic cracking. Appl Catal A-Gen 657, 119159. https://doi.org/10.1016/j.apcata.2023.119159.